Available online at www.sciencedirect.com
ScienceDirect
Trans. Nonferrous Met. Soc. China 25(2015) 3569−3577
Transactions of Nonferrous Metals Society of China
www.tnmsc.cn

Microstructural characterization and mechanical properties of functionally graded Al2024/SiC composites prepared by powder metallurgy techniques

F. ERDEMIR, A. CANAKCI, T. VAROL

Department of Metallurgical and Materials Engineering, Engineering Faculty,
Karadeniz Technical University, Trabzon 61000, Turkey

Received 19 December 2014; accepted 6 May 2015

Abstract: Al2024/SiC functionally graded materials (FGMs) with different numbers of graded layers and different amounts of SiC were fabricated successfully by powder metallurgy method and hot pressing process. The effects of increasing SiC content and number of layers of Al2024/SiC FGMs on the microstructure and mechanical properties of the composite were investigated. X-ray diffraction (XRD) and scanning electron microscopy (SEM) with energy-dispersive X-ray spectroscopy (EDX) analyses indicated that Al and SiC were dominant components as well as others such as Al_4C_3, $CuAl_2$, and $CuMgAl_2$. A maximum bending strength of 1400 MPa was obtained for two-layered FGMs which contained 40% SiC (mass fraction) on top layer. A decrease in microhardness and changes in porosity were discussed in relation to the SiC content and the intermetallics formation. The results show that the increase in microhardness values and intermetallic formation play a major role on the improvement of mechanical properties of the composites.

Key words: Al2024/SiC composites; functionally graded materials; intermetallics; microhardness; powder metallurgy

1 Introduction

Functionally graded materials (FGMs), a relatively new class of materials, have found a wide use in different fields such as automobile, aerospace, electronics, defense industries, gas turbine engines and engineering applications [1,2]. Functionally graded metal matrix composites (FGMMCs) are FGMs with metal and ceramic constituents, which are one of the most potential and prominent systems for the design and fabrication of components and structures with gradient properties. FGMMCs have superior capabilities for materials design and development of advanced engineering components. The specific properties obtained by the use of FGMMC are high temperature surface wear resistance, surface friction and thermal properties, adjusted thermal mismatching, reduced interfacial stresses, increased adhesion at metal−ceramic interface, minimized thermal stresses, increased fracture toughness and crack retardation [3,4].

Aluminum matrix composites (AMCs) are found to be potential materials because of their excellent physical, mechanical and tribological properties [5]. In recent years, attention has been paid for using AMCs as personal armor [6], where higher specific strength, stiffness and greater work hardening rate are important considerations. The mechanical properties of AMCs, such as toughness, strain rate deformation and dynamic loading strength, become very important when they are used as armor components. AMCs are usually more brittle than matrix materials and have lower fracture toughness. The dynamic fracture toughness of the aluminum matrix, which is reinforced with silicon carbide (SiC) and alumina (Al_2O_3) particulates, is higher than its static fracture toughness, but decreases as the volume fraction of the reinforcement increases [7−9]. The yield strength of SiC reinforced AMCs increases faster than that of un-reinforced aluminum [10]. SiC continuous network structure ceramics are a very promising material for use in semiconductor processing, nuclear fusion reactors, heat-sink plates, and high temperature thermo-mechanical applications because of their excellent chemical and thermal stability, high thermal conductivity, and good mechanical properties [11]. However, a problem of Al/SiC composites is that the microstructure shows a non-uniform distribution of SiC particles. The most significant detrimental property

Corresponding author: A. CANAKCI; Tel: +90-0462-377-2927; Fax: +90-0462-325-7405; E-mail: aykut@ktu.edu.tr
DOI: 10.1016/S1003-6326(15)63996-6

change may be the decrease in ductility and fracture toughness, which is true for all the AMCs and process histories, a major obstacle preventing their extensive use. The mechanism of reinforcement affecting the fracture toughness of AMCs is not well understood. Several models have been proposed to characterize the relationship between fracture toughness and microstructure [12]. This problem can be overcome by using FGMs. The composite material with sharp interface is replaced by layers of gradually changing microstructure and composition [13,14].

The fabrication process is one of the most important fields in FGM research. A large variety of production methods have been developed for the processing of FGMs, such as, powder metallurgy [15], thermal spray [16], slip casting [17], centrifugal casting [18], laser cladding [19] and chemical vapour deposition [20]. Powder metallurgy is considered as a good technique in producing metal−matrix composites. An important advantage of this method is its low processing temperature compared with melting techniques. On the other hand, good distribution of the reinforcing particles can be achieved [21]. Another advantage of powder metallurgy technique is its ability to manufacture near net shape product with low cost [22].

The beneficial effect of powder metallurgy on the production and properties of FGMs has been investigated by some researchers. In previous studies [23−26], powder metallurgy method has been used for the production of FGMs. However, to our knowledge, effect of the number of graded layers and SiC content on the microstructure and mechanical properties of Al2024/SiC FGMs has not been investigated. Therefore, the purpose of this work is to produce Al2024/SiC FGMs by powder metallurgy and hot pressing and to investigate effect of number of graded layers and SiC content on the microstructure, density, hardness and bending strength of the Al2024/SiC FGMs.

2 Experimental

The as-atomized Al2024 powders were supplied commercially with the chemical composition of 4.85% Cu, 1.78% Mg, 0.385% Si, 0.374% Fe, 0.312% Mn, 0.138% Zn, 0.042% Cr, 0.005% Ti (mass fraction) and Al as balance. Al2024 alloy powders with an average powder size of 54 μm were used as the matrix materials and SiC powders with an average particle size of 10 μm (Alfa Aesar, Germany) were used as the reinforcement material. Al2024 alloy powders, with different mass fractions of SiC powders (30%, 40%, 50%, and 60%) were blended in a planetary ball-mill (Fritsch Gmbh, model "Pulverisette 7 Premium line") at room temperature using a tungsten carbide bowl and a high argon atmosphere for 2 h in order to break up the hard agglomerates. The milling atmosphere was argon which was purged into a bowl before milling. The powder metallurgy method containing cold pressing followed by hot sintering was used for preparation of these composites. First layer of powder stocks was manually put successively in the die, and then the powder stock was uni-axially cold pressed in a die up to 250 MPa for 2 min. The punch was removed upward. The rest layers of powder stocks were manually put on the compacted first layers. The green compacts of Al2024/SiC FGMs samples in the die were hot pressed at 560 °C and 500 MPa in an argon atmosphere. Two-, three- and four-layered FGM samples were prepared for Al2024/SiC FGMs samples with 30%, 40%, 50% and 60% SiC. The sample designation and compositions of the FGMs samples are given in Table 1.

Table 1 Sample designation and composition of composites and functionally graded composites samples

Sample	Number of layer	Compositional gradient (Al2024/SiC)/%
A3	−	70/30
A4	−	60/40
A5	−	50/50
A6	−	40/60
AS3	2	100−70/30
AS4	2	100−60/40
AS5	2	100−50/50
AS6	2	100−40/60
AS34	3	100−70/30−60/40
AS45	3	100−60/40−50/50
AS56	3	100−50/50−40/60
AS345	4	100−70/30−60/40−50/50
AS456	4	100−60/40−50/50−40/60

The microstructure and elemental distribution of cross-section of FGMs were observed by means of a Zeiss Evo LS10 scanning electron microscope. For these purposes, the samples were sectioned first and then prepared with the standard metallographic technique. Mercury Intrusion Porosimetry (MIP) tests were performed on the FGMs samples after sintering. The equipment used for the MIP was an Autopore IV 9500 from Micromeritics which generates a maximum pressure of 414 MPa and can evaluate a theoretical pore diameter of 0.003 μm. The phase identification of the products was conducted by X-ray diffraction (Rigaku Corporation, Japan) using Cu K_{α} radiation. The microhardness of these composite samples was measured using the Vickers hardness (HV) method under a load of

1 kg for a dwell time of 15 s. The three-point bending test was performed using a MTS Universal Materials Testing Machine at room temperature. The crosshead speed was maintained at the speed of 0.5 mm/min. The geometry of three-point bending test sample is 6.6 mm × 10 mm × 45 mm.

3 Results and discussion

3.1 Microstructure

The typical microstructures of the Al2024/SiC composites and Al2024/SiC FGMs are presented in Fig. 1. In the microstructures, green colour represents the SiC ceramic particle and light gray colour represents the Al2024 matrix. The SiC particles are randomly dispersed in the Al2024 matrix for A3 sample as can be seen in Fig. 1(a). No clear evidence of heterogeneities in the distribution of SiC reinforcement particles is observed at the cross sections of these samples. Moreover, it is also observed that agglomeration of SiC particles within the Al2024 matrix cannot be avoided completely. It should be noted that a great number of SiC cluster may adversely result in non-homogeneity of the SiC distribution, as well as decreased physical and mechanical properties of the Al2024/SiC composites. The number of SiC cluster increased with increasing SiC content from 30% to 60% (Fig. 1(d)). It can be seen that porosity of A6 sample is higher than that of A3 sample. By comparison, obvious clusters increased in the A6 sample, which indicates that increasing SiC content could increase the porosity content. Figure 1(g) shows the microstructures of a cross-section of Al2024/SiC FGMs (AS4) with different interface details. The microstructure of interlayer changes from the Al2024 side to the Al2024/SiC side with the variation of composition. In other words, the microstructure of the system includes a compositional gradient change along the thickness direction, from pure Al2024 alloy to Al2024/SiC composites as can be observed from Fig. 1(g). It can be seen that both the Al2024 alloy and the composites are continuous in the microstructures. There are no indications of cracking within individual layers or decohesion at interfaces in any of the specimens as can be seen from the details of the microstructures for the different interfaces of the FGM (Fig. 1(g)). Moreover, there are no macroscopic interfaces in the FGMs. This good continuity of microstructure can eliminate the disadvantage of traditional macroscopic interfaces in metal/composite joints and reflects the design ideal of FGMs. No cracking between the layers can be found in the FGMs in this work (Figs. 1 and 2), indicating that the FGMs have good strength, good thermal stability and

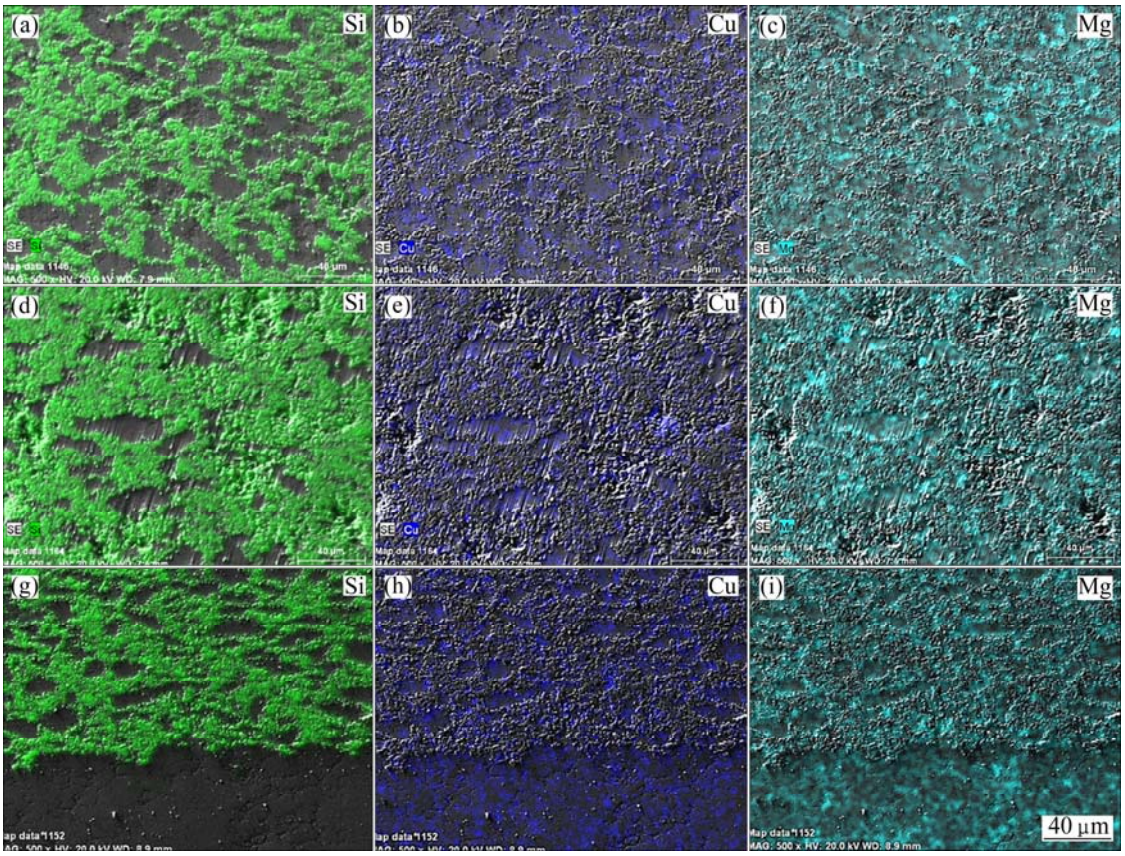

Fig. 1 SEM-EDX maps of Al2024/SiC composites and FGMs: (a−c) A3; (d−f) A6; (g−i) AS4 (In EDX maps, blue colour represents Cu, green colour is Si, turquoise blue colour is Mg and grey is Al)

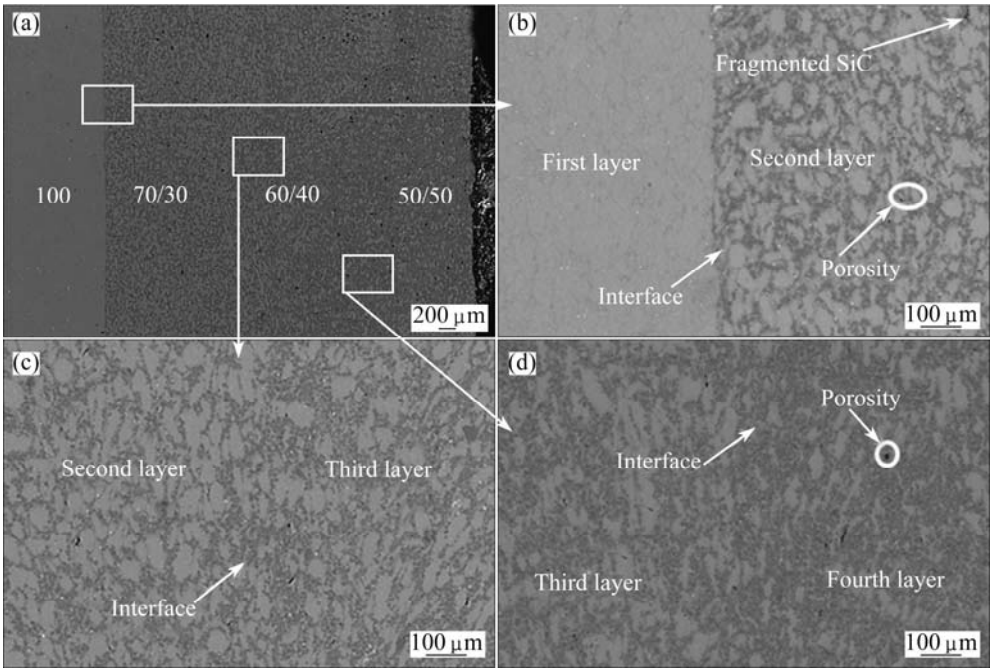

Fig. 2 SEM micrographs of AS345 composite sample

good thermal shock due to the better metal−ceramic bond, continuous microstructure at the interfaces of the FGMs, as reported in previous studies [27−30]. JIN et al [27] investigated properties of multilayered Mo-based FGMs fabricated by powder metallurgy. They stated that thermo-mechanical properties of Mo-based FGMs have gradient distribution corresponding to their composition. According to their study, the FGMs had better thermal shock resistance than the monolithic material. PINES et al [28] studied pressureless sintering of particle-reinforced metal−ceramic composites for FGMs. They reported that there are pores within the matrix that are decreased during hot pressing process due to the fact that there are pores associated with the agglomeration of reinforcing particles. KWON et al [29] produced carbon nanotubes (CNT) and nano-SiC reinforced aluminum matrix FGMs. They stated that Al/CNT/SiC and Al/CNT powder mixtures were fully compacted and demonstrated good adhesion with no serious micro-cracks and pores within FGMs.

In relation to EDX maps (Fig. 1), grey colour represents Al, blue colour is Cu, green colour is Si and turquoise blue colour is Mg. EDX maps are obtained from AS4 FGM sample (Figs. 1(g), (h) and (i)). As shown in Fig. 1(g), two-layered FGMs from Al2024 with grey region to Al2024/SiC with green regions are obviously distinguished. It can be observed that a significant increase in green region from bottom layer to top layer occurred with a change in the number of layer. It should be noted that SiC and Al are unsoluble in each other in solid state. So, SiC-rich regions can be shown at the Al2024 grain boundary. From EDX maps, Cu-containing phase of A3 composites such as Al_2Cu seems to have homogenous distribution and larger size than A6 composites. However, the distribution of the Al_2Cu phases is more homogenous in the AS4 samples. The decrease in size of Al_2Cu phases could be expected due to low cooling rates. So, the hot pressing process induces the dissolution of the Al_2Cu phase followed by its precipitation.

Figure 3 shows pore size distribution determined by means of MIP for the composite and FGM samples. A significant increase of the pore content of the composites sample from 0.5674 % to 2.0272 % with increasing SiC content from 30% to 60% was obtained. However, a significant reduction in the pore size from micrometer level to nanometer level is observed in MIP experiments as shown in Fig. 4(a). In other words, 60% SiC reinforced composites (A6) has the lowest density, which is mainly attributed to a higher content of SiC selected as reinforcement material. Between the composite samples, A3 sample has higher density than the other composite sample, because the SiC content within the Al2024 alloy matrix is lower. The higher density of sample A3 is mainly due to its higher densification ability and the less agglomeration regions. The porosity of FGM samples is considerably lower compared with the composite samples. This can be attributed to the effect of multiple pressing during the densification process. Depending on the number of layers, the number of the pressing also increases with increasing the number of layers. As it can be seen in Table 2, the pore content of Sample A6 is 2.0272%. The pore content is 0.2015% for AS6 sample. However, the porosity values trend to increase for three-

and four-layered Al2024/SiC composites (Table 2). This can be attributed to the increase in the numbers of agglomeration regions generated by hard SiC particles.

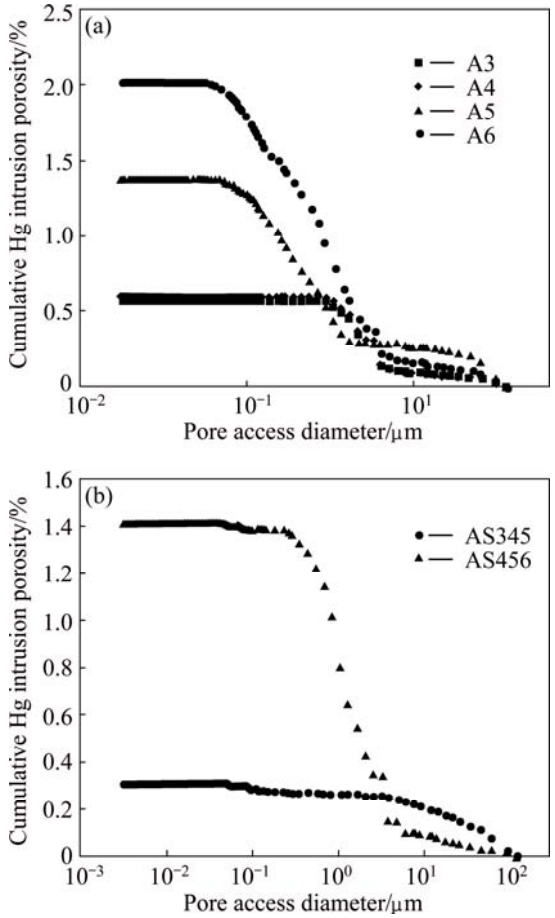

Fig. 3 Pore size distribution determined by means of MIP: (a) Samples A3, A4, A5 and A6; (b) AS345 and AS456 FGMs

3.2 Mechanical properties

The influence of the varying microstructures on the microhardness of the Al2024/SiC composites and FGMs sample is obvious, as shown in Table 2. As the content of SiC increases from 30% to 40%, the hardness changes and increases substantially. Under the same applied load during pressing, SiC particles in A4 composites are collided more rapidly than those in A3 composites. A more extensive plastic deformation in the A4 sample occurs. So, the higher stresses are produced at the Al2024/SiC reinforcement interface. This behavior can be ascribed to a dislocation mechanism in the metallic phase known as work hardening [30]. In other words, the reason for the highest hardness is due to work hardening. The randomly dispersed reinforcing particles (Fig. 1) at low SiC contents for A3 sample mainly causes the highest microhardness. An increase in the microhardness from HV 170 to HV 225 is observed with the change of microstructures to randomly dispersed particles for A3 and A4 samples, respectively. The increasing microhardness of these composites with the SiC content increasing can be attributed to the dispersion strengthening effect [31]. The average microhardness value is about HV 225 for A4 sample. It is clearly shown that the microhardness value of A4 sample is higher than those of A5 and A6 samples. The decrease in the microhardness values for A5 and A6 samples are due to agglomeration of reinforcing particles. The higher pore content was confirmed by MIP examination and lower intermetallic phase size. However, a significant increase in the pore content from 1.3811% to 2.0272% with change of microstructure from A5 to A6 samples is observed and the related microhardness drastically decreases down to HV 205 and HV 180. As compared with the Al2024 matrix, the microhardness of the composites is greater; moreover, the addition of reinforcement particles increases the hardness of the composites [32]. An increase in the microhardness of the FGMs with different mass fractions of reinforcement from the matrix to the reinforcement graded regions was also observed in previous investigations [27]. As compared with the A3 and AS3 samples, the hardness of the SiC graded region of FGM is greater. The reason for this higher microhardness is a decrease in the average pore content, as can be seen in Table 2. A decrease in the microhardness value from HV 170 to HV 132 occurs with a change in the number. Although the second layer of AS4 sample is composed of the agglomerated reinforcing particles, randomly dispersed SiC particles are observed on the third layer of AS345 samples as can be seen in Fig. 1(g) and Fig. 2. This level of reinforcement contributed is supported by other work considering microhardness of metals with particulate reinforcement [30]. This result supports the comparison performed by SHEN et al [33] that the particle distribution is a critical parameter regarding the hardness of Al-based composites.

The degree of bonding between the Al2024 matrix and SiC particles can be obtained by three-point bending tests. The bending strengths of the Al2024/SiC composites and FGMs sample are listed in Table 2. The load−deflection curves are obtained from the three-point bend tests of these composite samples. SiC reinforcement particles improve the bending strengths of the composite up to threshold value of SiC content. For A4 composites, the bending strength reaches 1052 MPa. The bending strengths of the A4 composites are higher than other composites. The reasons for the increase in hardness and bending strength are as follows: 1) the higher strength of the reinforcing phase; 2) the structure of the matrix alloy; 3) the semi-homogeneous dispersion of the reinforcing particles in the matrix; and 4) the good adhesion between the matrix and the reinforcement, strongly influenced by the consolidation method used. One of the most common failure mechanisms in AMCs is

Table 2 Density and bending strength for FGM and composite samples

Sample	Metal/ceramic (Al2024/SiC)	Microhardness (HV)	Average Microhardness (HV)	Porosity/%	Bending strength/ MPa
A3	70/30	170	170	0.5674	845
A4	60/40	225	225	0.5978	1052
A5	50/50	205	205	1.3811	940
A6	40/60	180	180	2.0272	914
AS3	100−70/30	90−174	132	0.061	860
AS4	100−60/40	96−230	163	0.1925	1400
AS5	100−50/50	100−210	155	0.2445	1342
AS6	100−40/60	105−185	145	0.2015	1169
AS34	100−70/30−60/40	108−180−238	175	0.5907	800
AS45	100−60/40−50/50	112−240−215	190	0.63	1185
AS56	100−50/50−40/60	115−217−190	174	0.6612	780
AS345	100−70/30−60/40−50/50	120−185−242−195	185	0.3059	723
AS456	100−60/40−50/50−40/60	125−245−195−192	190	1.4134	1000

debonding of the particle−matrix interface [20]. At higher SiC contents, the bending strength decreases. The bending strength decreases greatly from 1052 to 940 MPa although the content of SiC increases from 40% to 50%. These results can be explained by weak bonding between the Al2024 matrix and SiC reinforcement that produced using powder metallurgy method [21]. Weak interfacial bonding worsens the properties of AMCs and renders them useless in any application. The serious interfacial reactions between particles and matrix can cause the earlier failure of the particles. Because of these reasons, the particles are easily fractured near the main crack plane. In the latter, since more particles will be pulled out from the matrix, strength will decrease due to the low interfacial bond. And the pulled out particle lengths are longer. SEM observation for the composites exhibited optimum interfacial bond giving the highest strength. As seen in Table 2, the bending strength of two-layered FGMs is greater than the composites. An increase in the bending strength from 1052 to 1400 MPa for A4 and AS4 samples occur with a decrease in the pore content from 0.5978% to 0.1925%. 1400 MPa with the highest strength can be explained by the decreased average pore content of AS4 samples. While a significant increase in the pore content from 0.1925% to 0.2445% for AS4 and AS5 samples is detected, the bending strength decreases from 1400 to 1342 MPa.

Figure 4 shows the fracture surface of FGMs sample and matrix. Fracture path of AS45 sample is shown in Fig. 4(c). The microstructures involved in the fracture can be identified by the fracture path. The fracture of FGM sample dominantly propagated along the pores in matrix and interfaces. As can be seen in Fig. 4(a), SiC particles obstruct the formation of crack and cause crack deflection. Al2024 matrix becomes rigid with these particles. So, the bending strength increases. The crack deflection occurs while crack is propagating and reinforcement is achieved. The weak areas providing

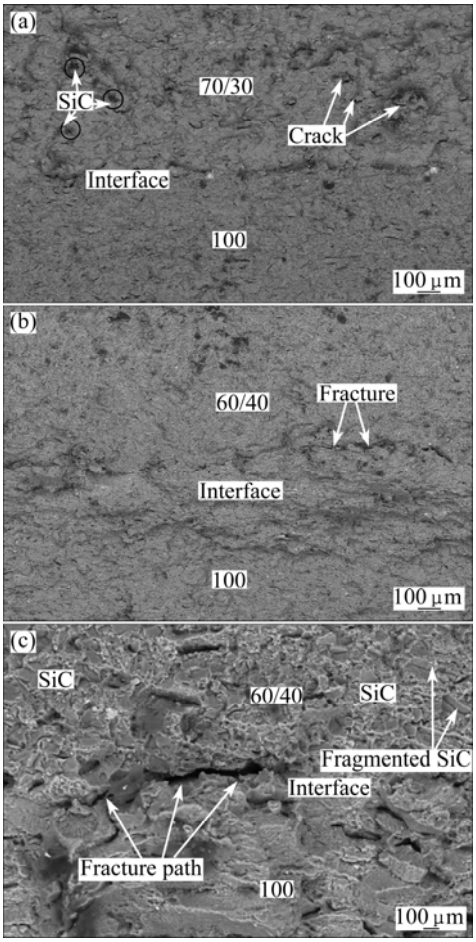

Fig. 4 Fracture surfaces of FGM samples: (a) AS3; (b) AS4; (c) AS45

less resistance to the impact were interface between layers. The results demonstrate that the fracture occurred at the pores in the Al2024 matrix. As compared to the AS3 and AS4 composites, AS4 has lower micro-crack (Fig. 4(b)). It is well known that the lower micro-crack means higher bending strength.

Figure 5 shows the load−deflection curves of FGM composites. These curves inform about crack propagation behavior of FGM composites. Up to point *A*, which is the first load drop on the load deflection curves, the load increases linearly and the samples exhibit elastic behavior in this regime. The reason for this load drop can be a crack initiation in layers of the FGM composite. The crack initiation in layers of the FGM composite is opened slowly from point *A* to point *B*, as can be seen in Fig. 5. In this regime, the elastic deformation occurs in the layers. At point *B*, which is the second drop, the load increases with deflection. The reason for the second load drop can be debonding at the FGM interface.

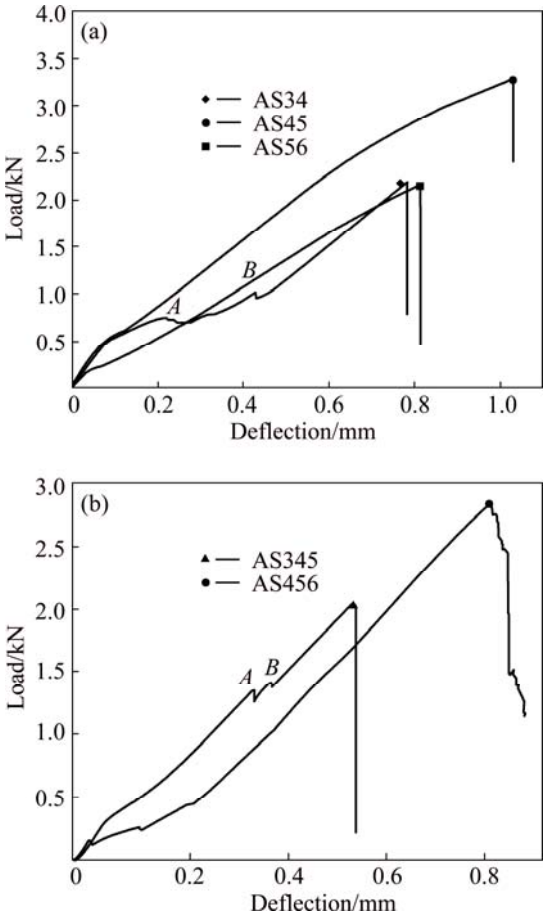

Fig. 5 Load−deflection curves obtained from three-point bend tests of FGM samples: (a) Three-layered FGM; (b) Four-layered FGM

3.3 XRD and EDX analyses

Figure 6 shows the SEM-EDX line profile with back scattered electron (BSE) image of the A4 composite samples. The line profile shows the distribution of SiC particle in the A4 composite. As shown in Fig. 6(a), the interface formed between SiC particle and Al2024 alloy reveals Al_4C_3 phases with bright regions. The result of EDX spot analysis demonstrated the presence of Al_4C_3.

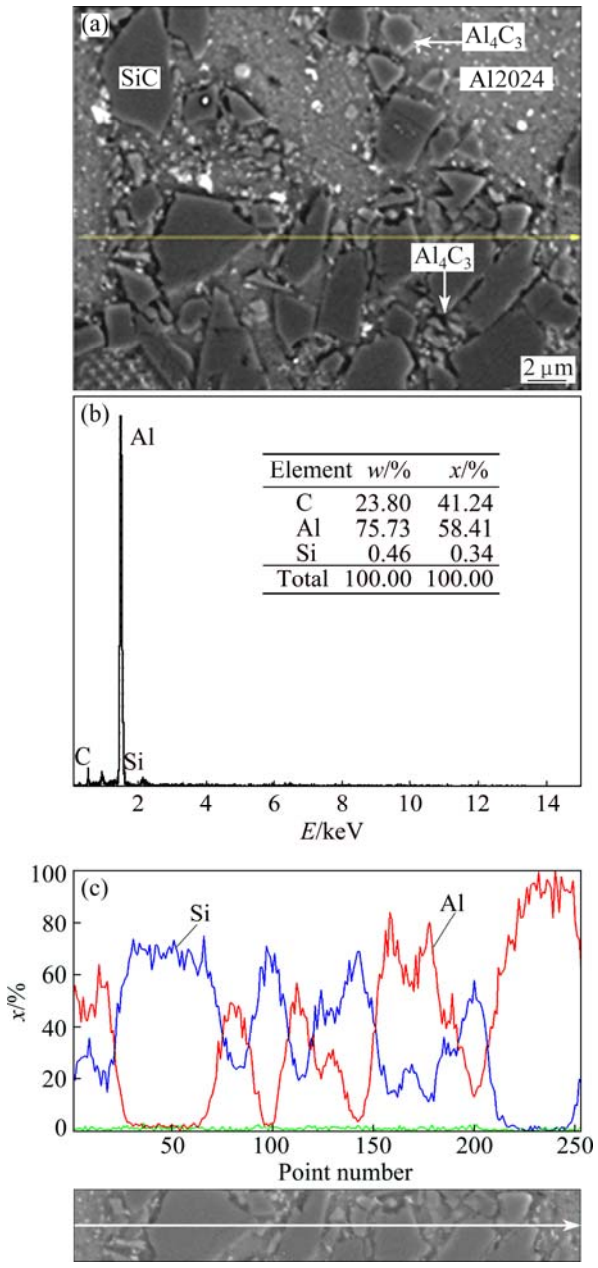

Fig. 6 SEM-EDX (indicated with green arrow) of A4 composite samples and its corresponding atom profiles: (a) Line profiles on morphology; (b) Point analysis; (c) Elemental distribution of Si and Al

XRD patterns of composite powders and composite samples are illustrated in Fig. 7. It can also be seen in the XRD pattern that there is a presence of Al and SiC, as well as other compounds such as Al_4C_3, $CuAl_2$, and $CuMgAl_2$. The XRD results support the SEM-EDX line scan and point analysis.

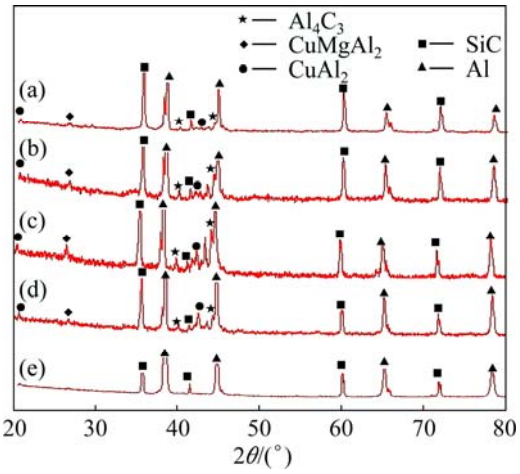

Fig. 7 XRD patterns of composites samples: (a) A6; (b) A5; (c) A4; (d) A3; (e) Mixed Al2024 and SiC powders

4 Conclusions

1) The porosity content of Al2024/SiC composites increases with the increase of SiC content. For 60% SiC, the porosity of the Al2024/SiC composites increases to about 2%. When Al2024/SiC FGMs with various numbers of graded layers are produced under the same conditions, the addition of layer has an important effect on porosity content.

2) The microhardness of the Al2024/SiC composite reinforced with 40% SiC reaches HV 225 in comparison to HV 170 of the Al2024/SiC composite reinforced with 30% SiC. However, for higher SiC contents (50% and 60%), the lower microhardness values are obtained due to increasing porosity content. The average microhardness of the Al2024/SiC FGMs increases with increasing the number of layer. The highest average microhardness of the FGMs coded as AS45 and AS456 is measured to be HV 190.

3) The bending strength firstly increases as the mass fraction of SiC increases from 30% to 40%, and then decreases as the mass fraction of SiC increases from 40% to 60% for Al2024/SiC composites. The decrease in the bending strength of the composites is due to the weakly bonded Al2024/SiC interface, less intermetallic formation, and lower microhardness values. The maximum bending strength obtained for AS4 composites is 1400 MPa.

4) The XRD patterns and SEM-EDX show the presence of compounds, such as Al_4C_3, $CuAl_2$, and $CuMgAl_2$ from the composites samples.

References

[1] VIEIRA A C, SEQUEIRA P D, GOMES J R, ROCHA L A. Dry sliding wear of Al alloy/SiCp functionally graded composites: Influence of processing conditions [J]. Wear, 2009, 267: 585−592.

[2] RECEP E, KEMAL A M, YILDIRIM M. Indentation behavior of functionally graded Al−SiC metal matrix composites with random particle dispersion [J]. Composite Part B: Engineering, 2011, 42: 1497−1507.

[3] MORTENSEN A, SURESH S. Functionally graded metals and metal–ceramic composites. Part 1: Processing [J]. International Materials Reviews, 1995, 40: 239−265.

[4] RAJAN T P D, PILLAI RM, PAI B C. Characterization of centrifugal cast functionally graded aluminum−silicon carbide metal matrix composites [J]. Materials Characterization, 2010, 61: 923−928.

[5] MONDAL D P, DAS S, RAO RN, SINGH M. Effect of SiC addition and running-in-wear on the sliding wear behaviour of Al−Zn−Mg aluminium alloy [J]. Materials Science and Engineering A, 2005, 402: 307−319.

[6] CHI R, SERJOUEI A, SRIDHAR I, TAN G E B. Ballistic impact on bi-layer alumina/aluminium armor: A semi-analytical approach [J]. International Journal of Impact Engineering, 2013, 52: 37−46.

[7] MARCHAND A, DUFFY J, CHRISTMAN T A, SURESH S. An experimental study of the dynamics mechanical properties of an Al−SiC_w composite [J]. Engineering Fracture Mechanics, 1988, 3: 295−315.

[8] SKOLIANOS S. Mechanical behaviour of cast SiC_p-reinforced Al−4.5%Cu−1.5%Mg alloy [J]. Materials Science and Engineering A, 1996, 210: 76−82.

[9] SURAPPA M K, SIVAKUMAR P. Fracture-toughness evaluation of 2040-Al/Al_2O_3 particulate composites by instrumented impact [J]. Composites Science and Technology, 1993, 46: 287−292.

[10] WANG Zhang-wei, SONG Min, SUN Chao, HE Yue-hui. Effects of particle size and distribution on the mechanical properties of SiC reinforced Al−Cu alloy composites [J]. Materials Science and Engineering A, 2011, 25: 1131−1137.

[11] LIM K Y, KIM Y W, KIM K J. Electrical properties of SiC ceramics sintered with 0.5 wt% AlN–RE_2O_3 [J]. Ceramics International, 2014, 40: 8885−8890.

[12] LIU Yong-sheng, CHAI Nan, QIN Hai-long, LI Zan, YE Fang, CHENG Lai-fei. Tensile fracture behavior and strength distribution of SiC_f/SiC composites with different SiBN interface thicknesses [J]. Ceramics International, 2015, 41: 1609−1616.

[13] MULLER E, DRASAR C, SCHILZ J, KAYSSER W A. Functionally graded materials for sensor and energy applications [J]. Materials Science and Engineering A, 2003, 362: 17−39.

[14] WU A H, CAO W B, GE C C, LI J F, KAWASAKI A. Fabrication and characteristics of plasma facing SiC/C functionally graded composite material [J]. Materials Chemistry and Physics, 2005, 91: 45−50.

[15] UBEYLI M, BALCI E, SARIKAN B, OZTAS M K, CAMUSCU N, YILDIRIM R O, KELES O. The ballistic performance of SiC-AA7075 functionally graded composite produced by powder metallurgy [J]. Materials and Design, 2014, 56: 31−36.

[16] PRCHLIK L, SAMPATH S, GUTLEBER J, BANCKE G, RUFF A W. Friction and wear properties of WC−Co and Mo−Mo_2C based functionally graded materials [J]. Wear, 2001, 249: 1103−1115.

[17] LOPEZ E S, BARTOLOME J F, PECHARROMAN C, MOYA J S. Zirconia/stainless-steel continuous functionally graded material [J]. Journal of the European Ceramic Society, 2002, 22: 2799−2804.

[18] ZHANG J, WANG Y Q, ZHOU B L. Functionally graded Al/Mg_2Si in-situ composites, prepared by centrifugal casting [J]. Journal of Materials Science Letters, 1998, 17: 1667−1679.

[19] MULLER P, MOGNOL P, HASCOET J Y. Modeling and control of a direct laser powder deposition process for Functionally Graded Materials (FGM) parts manufacturing [J]. Journal of Materials Science Letters, 2013, 213: 685−692.

[20] ASKARI E, MEHRALI M, METSELAAR I, KADRI N A, RAHMAN M. Fabrication and mechanical properties of Al_2O_3/SiC/ZrO_2 functionally graded material by electrophoretic deposition [J]. Journal of the Mechanical Behavior of Biomedical Materials, 2012, 12: 144−150.

[21] TORRALBA J M, DA COSTA C E, VELASCO F. P/M aluminum matrix composites: An overview [J]. Journal of Materials Processing Technology, 2003, 133: 203−206.

[22] MIN K H, KANG S P, KIM D G, KIM Y D. Sintering characteristic of Al_2O_3 reinforced 2xxx series Al composite powders [J]. Journal of Alloys and Compounds, 2005, 400: 150−153.

[23] KUMAR M S, CHANDRASEKAR P, CHANDRAMOHAN P, MOHANRAJ M. Characterisation of titanium−titanium boride composites processed by powder metallurgy techniques [J]. Materials Characterization, 2012, 73: 43−51.

[24] HE Z M, MA J, TAN G E B. Fabrication and characteristics of alumina–iron functionally graded materials [J]. Journal of Alloys and Compounds, 2009, 486: 815−818.

[25] BHATTACHARYYA M, KUMAR A N, KAPURIA S. Synthesis and characterization of Al/SiC and Ni/Al_2O_3 functionally graded materials [J]. Materials Science and Engineering A, 2008, 487: 524−535.

[26] NAI S, GUPTA M, LIM C. Synthesis and wear characterization of Al based, free standing functionally graded materials: Effects of different matrix compositions [J]. Composites Science and Technology, 2003, 63: 1895−1909.

[27] JIN G, TAKEUCHI M, HONDA S, NISHIKAWA T, AWAJI H. Properties of multilayered mullite/Mo functionally graded materials fabricated by powder metallurgy processing [J]. Materials Chemistry and Physics, 2005, 89: 238−243.

[28] PINES M L, BRUCK H A. Pressureless sintering of particle-reinforced metal–ceramic composites for functionally graded materials. Part I: Porosity reduction models [J]. Acta Materialia, 2006, 54: 1457−1465.

[29] KWON H, LEPAROUX M, KAWASAKI A. Functionally graded dual-nanoparticulate-reinforced aluminium matrix bulk materials fabricated by spark plasma sintering [J]. Journal of Materials Science and Technology, 2014, 30: 736−742.

[30] DÁVILA M M, PECH-CANUL M A, PECH-CANUL M I. Effect of bi- and trimodal size distribution on the superficial hardness of Al/SiCp composites prepared by pressureless infiltration [J]. Powder Technology, 2007, 176: 66−79.

[31] TOPCU I, GULSOY H O, KADIOGLU N. Processing and mechanical properties of B_4C reinforced Al matrix composites [J]. Journal of Alloys and Compounds, 2009, 482: 516−521.

[32] PURAZRANG K, ABACHI P, KAINER K U. Investigation of the mechanical behaviour of magnesium composites [J]. Composites A, 1994, 25: 296−302.

[33] SHEN Q, WU C, LUO G, FANG P, LI C, WANG Y, ZHANG L. Microstructure and mechanical properties of Al-7075/B_4C composites fabricated by plasma activated sintering [J]. Journal of Alloys and Compounds, 2014, 588: 265−270.

粉末冶金制备 Al2024/SiC 功能梯度复合材料的显微组织表征和力学性能

F. ERDEMIR, A. CANAKCI, T. VAROL

Department of Metallurgical and Materials Engineering, Engineering Faculty,
Karadeniz Technical University, Trabzon 61000, Turkey

摘　要：采用粉末冶金和热压技术制备了不同梯度层数和不同 SiC 含量的 Al2024/SiC 功能梯度材料。研究了梯度层数和 SiC 含量对 Al2024/SiC 功能梯度材料显微组织和力学性能的影响。XRD 和 SEM-EDX 分析表明 Al 和 SiC 为复合材料的主要成分，同时还有 Al_4C_3、$CuAl_2$ 和 $CuMgAl_2$ 等其他成分。表层含有 40% SiC 的两层 Al2024/SiC 功能梯度材料具有最高的抗弯强度，为 1400 MPa。显微硬度的降低和孔隙率的变化与 SiC 含量和金属间化合物的形成有关。结果表明，显微硬度的增加和金属间化合物的形成对复合材料力学性能的提高起重要作用。

关键词：Al2024/SiC 复合材料；功能梯度材料；金属间化合物；显微硬度；粉末冶金

(Edited by Yun-bin HE)